

Asymmetries in Foveal Vision

Samantha K. Jenks,^{1,2}  Marisa Carrasco,^{3,4} and Martina Poletti^{1,2,5}

¹Department of Brain and Cognitive Sciences, University of Rochester, Rochester, New York 14627, ²Center for Visual Science, University of Rochester, Rochester, New York 14627, ³Department of Psychology, New York University, New York, New York 10003, ⁴Center for Neural Science, New York University, New York, New York 10003, and ⁵Department of Neuroscience, University of Rochester, Rochester, New York 14627

Visual perception is characterized by known asymmetries in the visual field; human's visual sensitivity is higher along the horizontal than the vertical meridian, and along the lower than the upper vertical meridian. These asymmetries decrease with decreasing eccentricity from the periphery to the center of gaze, suggesting that they may be absent in the 1° foveola, the retinal region used to explore scenes at high-resolution. Using high-precision eyetracking and gaze contingent display, allowing for accurate control over the stimulated foveolar location despite the continuous eye motion at fixation, we investigated fine visual discrimination at different isoecentric locations across the foveola and parafovea in 12 human observers (both sexes). Although the tested foveolar locations were only 0.3° away from the center of gaze, we show that, similar to more eccentric locations, humans are more sensitive to stimuli presented along the horizontal than the vertical meridian. Whereas the magnitude of this asymmetry is reduced in the foveola, the magnitude of the vertical meridian asymmetry is comparable but, interestingly, the asymmetry is reversed: stimuli presented slightly above the center of gaze are more easily discerned than when presented at the same eccentricity below the center of gaze. Therefore, far from being uniform, as often assumed, foveolar vision is characterized by perceptual asymmetries. Further, these asymmetries differ not only in magnitude but also in direction compared to those present just ~4° away from the center of gaze, resulting in overall different foveal and extrafoveal perceptual fields.

Significance Statement

The 1° foveola, the retinal region responsible for high-resolution vision, has traditionally been studied as a uniform unit. Our research challenges this notion by uncovering perceptual asymmetries in foveolar fine spatial vision. Using a high-resolution eyetracker, we demonstrate that humans discriminate objects above the center of gaze better than below, a pattern opposite to the asymmetries observed just a few degrees away from the foveola. These findings reveal not only that this region is not uniform but also that it is not simply a high-resolution extension of extrafoveal vision but it is characterized by unique features. The discovery of these perceptual asymmetries raises critical questions about the neural representation of foveal input and the underlying factors shaping these differences.

Introduction

It is well established that perception across the visual field is not uniform. As eccentricity increases, visual acuity (Randall et al., 1966; Millodot et al., 1975; Westheimer, 1979), contrast sensitivity (Rijsdijk et al., 1980; Wright and Johnston, 1983; Jigo et al., 2023; Kwak et al., 2024), object recognition (Coates et al., 2013), and cortical magnification—the amount of cortical surface area corresponding to 1° of visual angle (Horton and Hoyt, 1991;

Himmelberg et al., 2021; Benson et al., 2022)—decline. Several factors contribute to this decline, including an increase in retinal cone (Curcio et al., 1987; Cooper et al., 2016; Reiniger et al., 2021) and retinal ganglion cell (Curcio et al., 1990; Watson, 2014) spacing, as well as an increase in the population receptive field (pRF) size in the visual cortex (Dumoulin and Wandell, 2008; Benson et al., 2018). It is, however, less known that vision is not uniform at isoecentric locations (polar angle) along a given eccentricity (see Himmelberg et al., 2023 for a review). In particular, sensitivity differs at isoecentric locations at the same eccentricity. This phenomenon is referred to as visual asymmetries (Carrasco et al., 2001; Cameron et al., 2002; Levine and McAnany, 2005; Fuller et al., 2008; Corbett and Carrasco, 2011; Abrams et al., 2012; Baldwin et al., 2012; Greenwood et al., 2017; Himmelberg et al., 2020; Hanning et al., 2024).

There are two well-studied visual asymmetries in the extrafoveal visual field: the *horizontal-vertical meridian asymmetry* (HVA), characterized by greater sensitivity along the horizontal

Received Jan. 9, 2025; revised May 29, 2025; accepted July 2, 2025.

Author Contributions: S.K.J. and M.P. designed research; S.K.J. performed research; S.K.J. and M.P. analyzed data; S.K.J. wrote the first draft of the paper; S.K.J. and M.P. wrote the paper; M.C. edited the paper.

This work was funded by NIH R01 EY029788-01 to M.P., NIH training grant T32EY007125 to S.K.J., EY001319 and NIH NEI Grant R01-EY-027401 to M.C.

The authors declare no competing financial interests.

Correspondence should be addressed to Martina Poletti at martina_poletti@urmc.rochester.edu.

This paper contains supplemental material available at: <https://doi.org/10.1523/JNEUROSCI.0055-25.2025>

<https://doi.org/10.1523/JNEUROSCI.0055-25.2025>

Copyright © 2025 the authors

than the vertical meridian, and the *vertical meridian asymmetry* (VMA), characterized by greater sensitivity along the lower than the upper vertical meridian (Carrasco et al., 2001; Cameron et al., 2002; Levine and McAnany, 2005; Fuller et al., 2008; Corbett and Carrasco, 2011; Abrams et al., 2012; Baldwin et al., 2012; Greenwood et al., 2017; Himmelberg et al., 2020; Jigo et al., 2023; Hanning et al., 2024; Kwak et al., 2024). These asymmetries have been assessed in many basic visual tasks, such as contrast sensitivity (Carrasco et al., 2001; Cameron et al., 2002; Fuller et al., 2008; Abrams et al., 2012; Himmelberg et al., 2020; Jigo et al., 2023; Kwak et al., 2024), texture segmentation (Talgar and Carrasco, 2002), and acuity (Wang et al., 2020; Barbot et al., 2021; Kwak et al., 2023). Interestingly, their extent increases with higher stimulus spatial frequency (Carrasco et al., 2001; Himmelberg et al., 2020; Barbot et al., 2021) and with increasing eccentricity from the center of gaze (Carrasco et al., 2001; Fuller et al., 2008; Baldwin et al., 2012; Jigo et al., 2023). It has also been shown that asymmetry is the strongest along the meridian, but gradually diminishes with angular distance from the meridian (Carrasco et al., 2001; Abrams et al., 2012; Baldwin et al., 2012; Barbot et al., 2021). These changes create a continuous field of gradually varying sensitivity, referred to as the performance field (Mackeben, 1999; Carrasco et al., 2001; Cameron et al., 2002).

Visual asymmetries have also been reported in more complex tasks such as letter identification task (Mackeben, 1999) visually guided pointing (Danckert and Goodale, 2001), motion discrimination (Fuller and Carrasco, 2009), numerosity (Chakravarthi et al., 2022), perceived size (Schwarzkopf, 2019), and visual short-term memory (Montaser-Kouhsari and Carrasco, 2009). Furthermore, visual asymmetries persist even when spatial attention—both exogenous (Carrasco et al., 2001; Cameron et al., 2002; Talgar and Carrasco, 2002; Roberts et al., 2016, 2018) and endogenous (Purokayastha et al., 2021; Tünçök et al., 2025a)—or temporal attention (Fernández et al., 2018) is engaged. Therefore, visual asymmetries are pervasive and shape multiple aspects of visual processing.

Many studies have examined visual asymmetries in the extra-foveal visual field, yet it is unknown whether they extend to the foveola. The foveola receives input from the central 1° of the visual field (Kolb et al., 1995). This region is responsible for high-resolution vision; it is defined by being devoid of capillaries and rods, and it is characterized by the highest cone density and spatial resolution. Therefore, the foveola is of paramount importance in many everyday tasks such as reading, driving, and discriminating stimuli from a distance. Further, although the foveola covers <0.01% of the visual field, its input is overrepresented by ≈ 800 times in the primary visual cortex (Azzopardi and Cowey, 1993). Yet, foveolar vision is often assumed to be characterized by uniformly high sensitivity and is generally treated as a single homogeneous region.

Based on evidence that the magnitude of visual asymmetries decreases at near eccentricities (Carrasco et al., 2001; Fuller et al., 2008; Baldwin et al., 2012; Jigo et al., 2023) and that spot-light sensitivity for isoeccentric locations in the foveolar field is uniform (Domdei et al., 2021), we may expect no asymmetries in visual discrimination within the central 1° of the visual field, where acuity, under normal viewing conditions, is primarily limited by uniform optics (Liang et al., 1997; Atchison et al., 2006; Bedgood et al., 2008). However, evidence showing that fine spatial vision already starts to decline across the central fovea (Poletti et al., 2013; Intoy and Rucci, 2020), and that retinal cone density along the vertical meridian of the foveola declines with

eccentricity more pronouncedly than along the horizontal meridian (Curcio et al., 1987, 1990; Reiniger et al., 2021) would suggest otherwise.

Assessing visual asymmetries at the foveolar scale requires precise localization of the line of sight, with arcminute level accuracy, to present small stimuli at predefined eccentricities from the preferred locus of fixation, a capability that exceeds what commercial video-eyetrackers can achieve (Holmqvist and Blignaut, 2020). To overcome these issues and investigate fine visual discrimination at isoeccentric locations in the foveola, we relied on a custom-made high-precision digital Dual Purkinje Image eyetracker (Wu et al., 2023) coupled with a gaze contingent display system (Santini et al., 2007). Together, these systems enable the recording of eye movements with high-precision and provide a more accurate localization of the line of sight (Poletti and Rucci, 2016; Wu et al., 2023).

Methods

Subjects. The experiment included 13 participants (11 naïve), including one of the authors, aged 18 or older (mean 24 ± 4.54 years; 8 female) with normal or corrected to normal vision. One subject was removed from the analysis due to performance being at chance level in all conditions tested. Eight of the 12 subjects participated in both conditions (foveola, $n = 12$ and parafovea $n = 8$). The University of Rochester Institutional Review Boards approved the experiment. All study participants provided consent prior to the study. Two subjects exhibited relatively large gaze instability during fixation, which would have led to the exclusion of too many trials under our original selection criteria—specifically, requiring gaze to remain within 10 arcmin of the central fixation point during the period of interest in the foveola condition. Rather than exclude these subjects entirely, we opted to test them using retinal stabilization. This approach allowed us to present stimuli at the intended retinal location despite the presence of large drifts. All trials in the foveola condition for these two subjects were conducted under retinal stabilization. These subjects are marked by triangles and dashed lines in the figures.

Apparatus. Stimuli were displayed on an LCD monitor with a refresh rate of 200 Hz and a spatial resolution of 1920×1080 pixels (Acer Predator XB272). The task was performed monocularly with the right eye while the left eye was patched. To prevent head movements, a unique dental-imprint bite bar and a headrest were used. The first and fourth Purkinje images of the right eye were captured at 340 Hz using a high-precision digital Dual Purkinje Image eyetracker (Wu et al., 2023). The position of the images were then sent to EYERIS—a custom-developed software that allows for flexible gaze contingent display control (Santini et al., 2007)—which processes eye movements in real time, and updated the stimulus on the display based on the desired combination of estimated oculomotor variables.

System calibration. Before the start of each block, subjects align their unique dental-imprint bite bar to the center of monitor, by looking through a set of two pinholes. Once aligned, the subject undergoes two step system calibrations. First, subjects undergo a standard automatic calibration procedure using a 3×3 grid of points. Points were 1.32° apart from each other in the horizontal and vertical directions. The mapping obtained through the automatic calibration was then refined using a custom-made manual calibration procedure (Poletti et al., 2013; Poletti and Rucci, 2016). This dual-step calibration allows a more accurate localization of gaze position than standard single-step procedures, improving 2D localization of the line of sight by approximately a factor of three on each axis (Poletti et al., 2013; Poletti and Rucci, 2016). During the experiment, the manual calibration procedure was then repeated for the central fixation marker before each trial to compensate for possible small head movements introducing errors in gaze localization.

Experimental protocol. After calibration, subjects started the trial by pressing a button. The stimulus array consisted of four 7×7 arcmin squares

at 0.33° (foveola condition) or 22×22 arcmin squares at 4.5° (parafovea condition) away from the central fixation square (5×5 arcmin). These placeholders could be either located along the cardinal directions or along four intercardinal directions. Cardinal and intercardinal directions were tested in separate blocks for a total of eight tested locations. While subjects maintained fixation on a central marker, a small bar (2×7 arcmin or 6×20 arcmin) tilted $\pm 45^\circ$ was briefly presented for 50 ms at one of four possible locations. The parafoveal stimuli were magnified according to the cortical magnification factor at that eccentricity (Rovamo and Virsu, 1979), similarly to the way is calculated in prior studies (Covey and Rolls, 1974; Strasburger et al., 1994; Carrasco and Frieder, 1997; Jigo et al., 2023). Subjects performed a two-alternative forced choice orientation discrimination task. Stimuli contrast was adjusted using the method of constant stimuli during a preliminary session to yield an overall performance of 70% correct responses across the eight locations tested. Stimuli contrast was then maintained at this level throughout the following experimental sessions. After 250 ms from target offset, a green response cue (2×7 arcmin or 6×20 bar) appeared for 100 ms. Subjects had 4 s to report the orientation of the target stimulus using a joystick.

Analysis of oculomotor data. For all subjects, only trials with optimal, uninterrupted tracking were selected. Further, trials with microsaccades occurring from 100 ms before target onset to 250 ms after target offset (400 ms microsaccade-free window), and trials with saccades occurring from 400 ms before target onset to 250 ms after target offset (700 ms saccade-free window), were discarded (see also Fig. S1). For the two participants who viewed the foveal stimuli under retinal stabilization in the foveola condition, trials characterized with drift amplitudes larger than 100 arcmin were removed to eliminate instances in which subjects attempted to chase the stabilized stimulus (0.2% of trials for subject 1 and 1.2% for subject 2). With the exception of two subjects in the foveola condition, the rest of the subjects, in that condition, and all the subjects in the parafovea condition viewed stimuli without retinal stabilization. For the subjects viewing the stimuli without retinal stabilization in the foveola condition, trials in which the gaze was ≥ 10 arcmin away from the central fixation marker during the period of interest (50 ms before target onset to 50 ms after target offset) were discarded to ensure that stimuli were presented at the desired eccentricity (see Methods; on average $10\% \pm 7\%$ of trials were removed for this reason). This criterion was more relaxed in the Parafoveal condition, as the stimuli were farther away from the center of gaze. Trials in which gaze was ≥ 30 arcmin away from the central fixation marker during the period of interest were discarded (on average $2\% \pm 1\%$ of trials).

Although prior studies have ruled out the influence of microsaccades on extrafoveal perceptual asymmetries (Purokayastha et al., 2021; Palmieri et al., 2023), oculomotor activity may still impact performance at the foveal level. Saccades are known to enhance perceptual performance at their target location, whether the stimulus appears before (Deubel and Schneider, 1996) or after the saccade (Hanning et al., 2016; Ohl et al., 2024). Similarly, microsaccades have been shown to facilitate perception both extrafoveally (Hafed, 2013; Hafed et al., 2015) and at the fovea (Shelchkova and Poletti, 2020; Guzhang et al., 2024). To minimize these potential confounds, we enforced a 400 ms microsaccade-free window around target presentation and conducted additional analyses to confirm that our results were not influenced by oculomotor events occurring outside this window. These control analyses are detailed in the supplementary material (Figs. S1–S3).

Analysis of behavioral data and statistics. Besides characterizing performance as percent of correct responses, we also calculated performance as d -prime. Hit and false alarm rates were corrected for response bias (Stanislaw and Todorov, 1999). Overall, we found the results based on the d -prime performance in agreement with those based on percent correct reported in the main text. Both conditions, showed a significant HVA; participants were on average $58\% \pm 24\%$ better at discriminating stimuli along the horizontal than the vertical meridian in the parafovea [horizontal = $3 d' \pm 1 d'$; vertical = $0.75 d' \pm 0.4 d'$; two-tailed paired t -test: $t(7) = 5.43$, $p = 0.0001$; BF = 41.96; Cohen's $d = 2.86$], and $15\% \pm 18\%$ and better in the foveola [horizontal: $1.34 d' \pm 0.41 d'$; vertical: $0.97 d' \pm 0.28 d'$; two-tailed paired t -test: $t(11) = 2.69$, $p = 0.021$; BF = 3.28;

Cohen's $d = 0.98$]. Additionally, our findings show that the sensitivity in the lower vertical meridian was higher than in the upper vertical meridian [lower: $1.12 d' \pm 0.5 d'$ upper: $0.42 d' \pm 0.42 d'$; two-tailed paired t -test: $t(7) = -4.94$, $p = 0.002$; BF = 27.05; Cohen's $d = 1.35$]. Again, this pattern was reversed in the foveolar condition; the upper vertical meridian was more sensitive than the lower vertical meridian [upper: $1.36 d' \pm 0.42 d'$ vs lower: $0.67 d' \pm 0.38 d'$; two-tailed paired t -test: $t(11) = 4.46$, $p = 0.001$; BF = 41.15; Cohen's $d = 1.58$].

All analyses were performed in MATLAB. ANOVAs, post hoc multiple comparison tests, paired t -tests, and Cohen's d calculations were performed using MATLAB's statistical toolbox. The Bayes Factor for ANOVA's and t -tests was calculated using the Bayesfactor MATLAB toolbox (<https://zenodo.org/badge/latestdoi/10.12604/7070>).

Results

Visual asymmetries are defined as differences in visual perception (e.g., visual sensitivity and acuity) at different polar angles along a given eccentricity. Whereas asymmetries in the parafovea and perifovea have been extensively studied, it is not yet known whether asymmetries are present in the 1° central fovea. To investigate this issue, fine spatial discrimination was tested at eight isoecentric locations in the foveola (four cardinal and four intercardinal), ≈ 20 arcmin away from the preferred locus of fixation (foveolar condition, Fig. 1A,B). As a comparison, performance was also assessed at the corresponding locations in the parafovea at 4.5° eccentricity (parafoveal condition). Observers were asked to maintain fixation on a central marker while discriminating the orientation of a tiny bar (tilted $\pm 45^\circ$) that was briefly presented at one of the tested locations (Fig. 1A). To maintain comparable task difficulty between the foveal and parafoveal conditions, stimulus contrast was adjusted to yield an overall performance $\approx 70\%$ of correct responses across the eight tested locations in each condition [$t(7) = -0.61$, $p = 0.56$, paired two-tailed t -test; BF = 2.54 for the null hypothesis; Fig. 1C].

Testing fine spatial vision within the foveola is challenging because it is difficult to present and maintain stimuli at the desired location, only arcminutes away from the preferred locus of fixation. During fixation, eye movements continually shift the retinal projections of objects across the foveola, even during brief fixation periods (Cherici et al., 2012; Rucci and Poletti, 2015). Here, we used a high-precision eyetracker (Wu et al., 2023) and a gaze contingent display (Santini et al., 2007) to more accurately localize the line of sight and to either present stimuli at a fixed eccentricity using retinal stabilization, or to post hoc select only trials in which gaze position was maintained within a circular region of 10 arcmin in radius around the center of the display ($10\% \pm 7\%$ of trials in the foveola were removed post hoc for gaze off center). Figure 1D shows that in the latter case, the average target distance from the preferred locus of fixation remained approximately at the desired eccentricity of $20' \pm 3'$, and it was comparable across all tested locations [$N = 10$, $F(7, 9) = 1.93$, $p = 0.08$, one-way ANOVA; BF = 1.56 for the null hypothesis]. Retinal stabilization was used only for two subjects who showed larger fixational instability (see Methods for details).

Despite the stimuli being presented at isoecentric locations, performance was not uniform across the eight tested locations both in the parafovea [$F(7, 7) = 12.21$, $p < 0.0001$, one-way ANOVA; BF > 100] and in the foveola [$F(7, 11) = 4.95$, $p = 0.0001$, one-way ANOVA; BF > 100]. Consistent with previous literature (Mackeben, 1999; Carrasco et al., 2001; Cameron et al., 2002; Baldwin et al., 2012; Schwarzkopf, 2019; Barbot et al., 2021; Chakravarthi et al., 2022), in the parafoveal condition, we found the typical HVA in performance; subjects were on average $27\% \pm 12\%$ better at discriminating stimuli

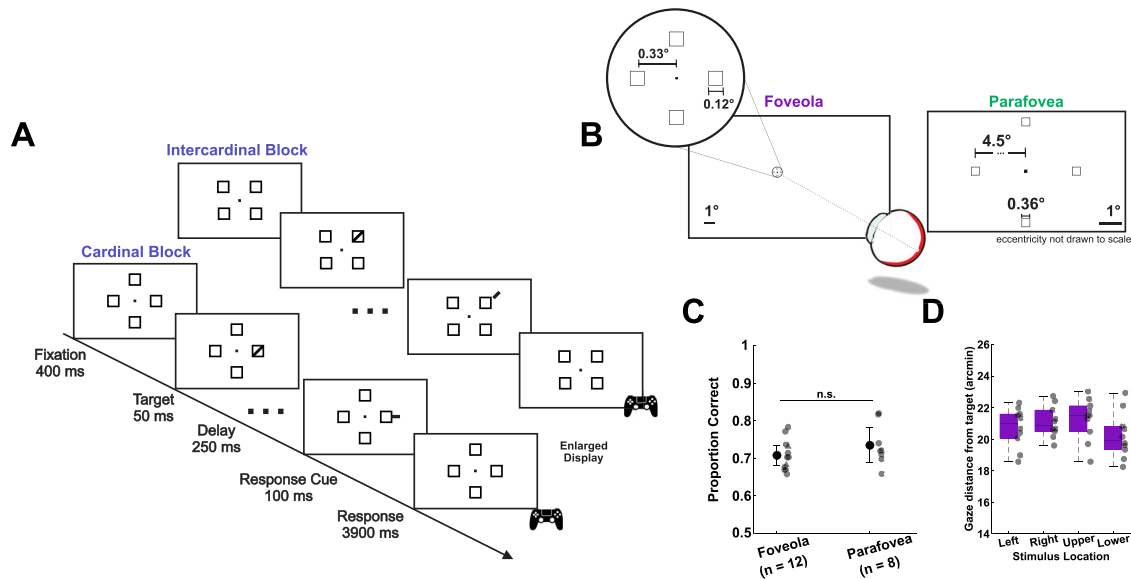


Figure 1. Experimental protocol. **A**, Subjects fixated monocularly (left eye patched) on a central fixation marker while stimuli were presented. The target, a small bar tilted $\pm 45^\circ$, appeared briefly (50 ms) at one of four possible locations and subjects were asked to report its orientation once the response cue was presented. A total of eight locations were tested. Cardinal and intercardinal locations were tested in separate blocks. **B**, Stimuli spatial arrangement and dimensions in the foveola (left; $n = 12$) and parafovea (right; $n = 8$) conditions. In the latter condition, stimuli were magnified according to the cortical magnification factor (Rovamo and Virsu, 1979). **C**, In a preliminary session, the stimulus contrast was determined for the foveola and the parafovea conditions separately, so that overall performance across cardinal and intercardinal locations yielded $\approx 70\%$ correct responses. Error bars are 95% confidence intervals. **D**, The target was 20 arcmin from the center of the display. The box and whisker plot shows that the average gaze distance from the target was approximately 20 arcmin for different target locations in the foveola condition. Triangles represent the two subjects under conditions of retinal stabilization (see Methods for detail). Error bars are 95% confidence intervals.

along the horizontal than the vertical meridian [Fig. 2A,B; horizontal = $91\% \pm 4\%$; vertical = $64\% \pm 3\%$; two-tailed paired t -test: $t(7) = 6.37$, $p = 0.0004$; BF = 91.22; Cohen's $d = 3.44$]. Interestingly, when stimuli were presented foveally, a similar pattern was found [Fig. 2A; horizontal: $74\% \pm 4\%$; vertical: $68\% \pm 3\%$; two-tailed paired t -test: $t(11) = 2.71$, $p = 0.02$; BF = 3.36; Cohen's $d = 0.94$]. This asymmetry was present for all individual subjects in the parafovea and for most subjects in the foveola (Fig. 2B). We then quantified the magnitude and direction of the asymmetry by computing the difference in overall performance along the vertical versus horizontal meridian, divided by the sum of performance across these two meridians (Tünçöğ et al., 2025b). The absolute value of this ratio reflects the magnitude of the asymmetry, while the sign indicates its direction. Our results show that the magnitude of this asymmetry was 4.4 times larger in the parafovea than in the central fovea [unpaired t -test: $t(18) = 4.77$, $p < 0.001$; BF > 100, Cohen's $d = 1.66$; Fig. 2C]. These results are consistent with the findings that asymmetries increase with eccentricity (Carrasco et al., 2001; Baldwin et al., 2012; Jigo et al., 2023). To further assess the difference between the foveal and parafoveal HVA, we compared the behavioral performance for the HVA with a two-way repeated measures ANOVA, excluding the four subjects who did not have data for the parafovea condition (asymmetry: horizontal vs vertical meridian, and eccentricity: fovea vs parafovea). We found significant main effects of asymmetry [$F(1, 7) = 25.73$, $p = 0.0014$] and eccentricity [$F(1, 7) = 7.68$, $p = 0.028$]. Further, there was an interaction [$F(1, 7) = 35.90$, $p < 0.001$] between eccentricity and asymmetry. A Tukey's post hoc test revealed a more pronounced HVA for parafoveal than foveal conditions ($p = 0.028$).

In the parafoveal condition, both locations along the vertical meridian showed a significant drop in performance compared to those along the horizontal meridian [$F(2, 7) = 37.33$, $p < 0.0001$; BF = 5.51; horizontal: $91\% \pm 4\%$; lower vertical: $70\% \pm 7\%$; upper vertical: $58\% \pm 7\%$]. However, in the foveola

condition, the HVA was mainly the result of a drop in performance in the lower vertical meridian [$F(2, 11) = 13.29$, $p = 0.0002$; BF = 106.35; horizontal: $74\% \pm 4\%$; lower vertical: $63\% \pm 4\%$; upper vertical: $74\% \pm 7\%$; Fig. 2D].

There was no statistically significant difference in reaction times for stimuli presented along the vertical vs horizontal meridian in the foveola ($Z = -1.2990$, $p = 0.1939$, Wilcoxon rank-sum test), and in the parafovea reaction times were faster for stimuli presented along the horizontal meridian (horizontal: 367 ± 125 ms; vertical: 524 ± 180 ms; $Z = -2.15$, $p = 0.031$, Wilcoxon rank-sum test), indicating that the reported asymmetries in visual discrimination are not due to a speed accuracy trade-off.

Besides the horizontal-vertical asymmetry, differences in visual perception are also reported along the vertical meridian. Previous research has consistently shown that in the parafovea and periphery sensitivity is higher in the lower than the upper vertical meridian (Carrasco et al., 2001; Cameron et al., 2002; Montaser-Kouhsari and Carrasco, 2009; Abrams et al., 2012; Himmelberg et al., 2020; Barbot et al., 2021; Hanning et al., 2022; Kwak et al., 2023; Jigo et al., 2023; Tünçöğ et al., 2025a; Kwak et al., 2024). Our findings in the parafovea are in line with the literature [Fig. 3A,B; lower: $70\% \pm 7\%$ upper: $58\% \pm 7\%$; two-tailed paired t -test: $t(7) = -4.90$, $p = 0.002$; BF = 26.21; Cohen's $d = 1.35$].

We then quantified the magnitude and direction of the VMA by computing the difference in overall performance between the upper and lower vertical meridian locations, divided by the sum of performance across these locations (Tünçöğ et al., 2025b). The absolute value of this ratio reflects the magnitude of the asymmetry, while the sign indicates its direction. In the central foveola, we reported an asymmetry of comparable magnitude to what found extrafoveally [VMA foveola vs VMA parafovea: unpaired t -test, $t(18) = 0.36$, $p = 0.73$; BF = 2.38 for the null hypothesis, Cohen's $d = 0.071$; fovea: $11\% \pm 9\%$ and parafovea: $12\% \pm 7\%$], indicating that not all asymmetries are attenuated

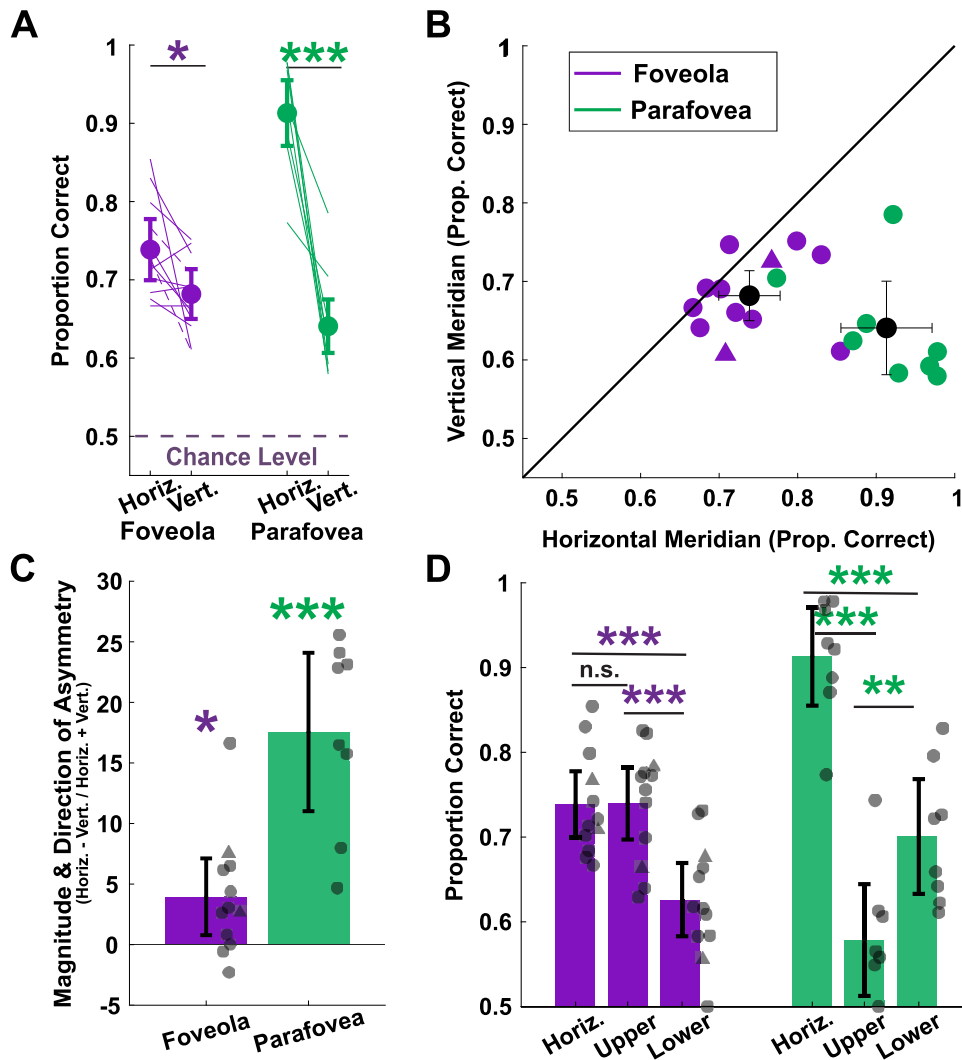


Figure 2. Horizontal–vertical meridian asymmetry. **A** and **B**, Average performance along the horizontal (pooled left and right locations) and vertical meridian (pooled top and bottom locations) across subjects for the foveola and the parafovea. In **A**, lines represent individual observers; the two observers who viewed stimuli under retinal stabilization conditions are marked by dashed lines. Asterisks denote a statistically significant difference (* $p < 0.05$, ** $p \leq 0.01$, *** $p \leq 0.001$, paired t -test $p = 0.02$ foveola, $p = 0.0004$ parafovea). **C**, Magnitude and direction of the horizontal–vertical meridian asymmetry. Asterisks indicate a statistically significant difference from zero (one sample t -test $p = 0.02$ foveola, $p = 0.0004$ parafovea). **D**, Average performance along the horizontal meridian compared to the upper and lower vertical meridian performance for the foveola and the parafovea. Asterisks denote statistically significant differences (one-way ANOVA, $p = 0.0001$ foveola, $p < 0.0001$ parafovea). All Error bars are 95% confidence intervals. Triangles represent the two observers tested under conditions of retinal stabilization (see Methods for detail).

in this region. Remarkably, the pattern of asymmetry reversed in the foveola (Fig. 3C); visual discrimination was better in the upper than the lower vertical meridian [upper: $73\% \pm 4\%$ vs lower: $63\% \pm 4\%$; two-tailed paired t -test: $t(11) = 4.32$, $p = 0.001$; BF = 34.07; Cohen's $d = 1.56$]. Once the directionality of the VMA was considered, a statistically significant difference was present between foveola and parafovea [VMA foveola vs VMA parafovea: unpaired t -test, $t(18) = 6.16$, $p < 0.001$; BF > 100 for the null hypothesis, Cohen's $d = 2.76$], indicating that, although the magnitude was comparable, the direction of the asymmetry was reversed in the foveola. Further, when comparing reaction times in the lower and upper vertical meridians for the foveola and parafovea, there was no statistically significant difference (foveola: $Z = -1.18$, $p = 0.24$; parafovea: $Z = 0.9977$, $p = 0.32$, Wilcoxon rank-sum test), indicating that the results were not due to a speed-accuracy trade-off.

To further compare the behavioral performance for the VMA between the foveola and the parafovea, we performed a two-way

repeated measures ANOVA (asymmetry: upper vs lower and eccentricity: fovea vs parafovea) excluding the four subjects who did not have data for the parafovea condition. Given the presence of a balanced crossover effect in the results, the main effects of asymmetry and eccentricity were not significant. However, there was a statistically significant interaction between visual field (upper vs lower) and eccentricity [$F(1, 7) = 26.76$, $p = 0.0013$], indicating that although the magnitude of the VMA was comparable at the two tested eccentricities, the direction of the asymmetry was opposite.

To examine the visual performance fields with finer resolution, visual discrimination was also tested at intercardinal locations. As reported in some studies (Carrasco et al., 2001; Corbett and Carrasco, 2011; Abrams et al., 2012; Barbot et al., 2021), the most noticeable feature of the parafovea and perifovea performance field was the enhancement of performance along the horizontal meridian, giving the performance field an oblong shape (Fig. 4A). The performance field in the central fovea, in

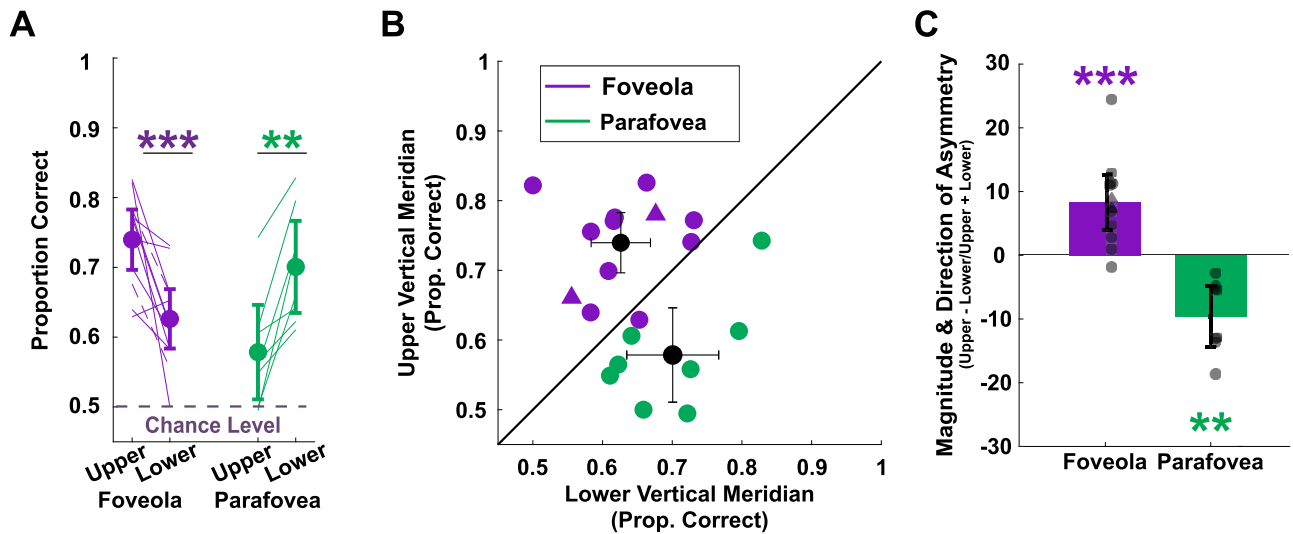


Figure 3. Vertical meridian asymmetry. Conventions are the same as in Figure 2. **A** and **B**, Average performance along the upper and lower vertical meridian across subjects. In **A**, asterisks denote a statistically significant difference (paired *t*-test, $p = 0.001$ foveola, $p = 0.002$ parafovea). **C**, Magnitude and direction of the vertical meridian asymmetry. Asterisks indicate a statistically significant difference from zero (one sample *t*-test, $p = 0.001$ foveola, $p = 0.002$ parafovea). All error bars are 95% confidence intervals.

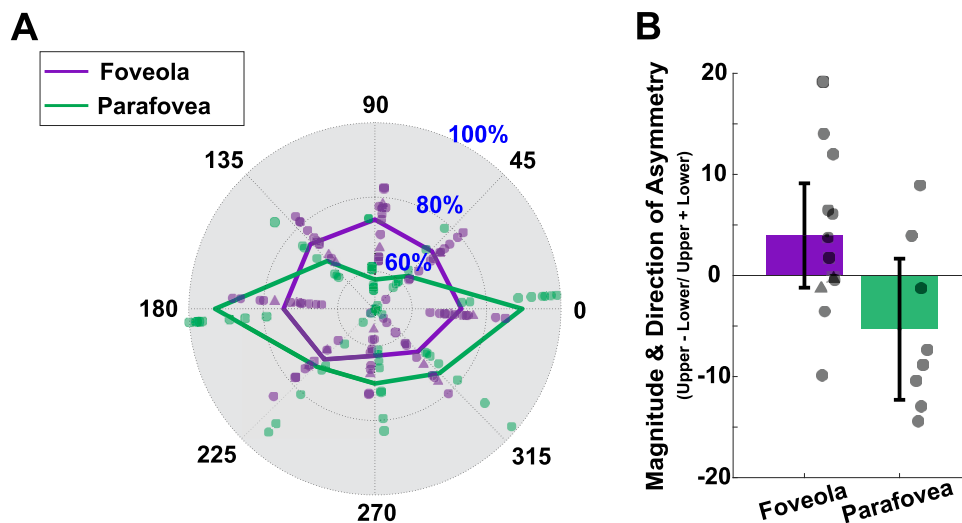


Figure 4. Performance fields in the foveola and parafovea. **A**, The visual performance field in the foveola (purple) and parafovea (green). Each angle represents one tested location. Numbers along the radial direction represent percent correct, and the shaded regions represent SEM. The lines connect the average performance across subjects for the different locations tested. **B**, Magnitude and direction of the asymmetry between the upper intercardinal locations (locations at 45° and 135°) and the lower intercardinal locations (locations at 225° and 315°). Error bars are 95% confidence intervals. Triangles represent the two subjects tested under conditions of retinal stabilization (see Methods for detail).

contrast, is less oblong and it is mainly characterized by an upper vertical meridian enhancement (Fig. 4A). Performance between the upper and lower intercardinal locations were comparable for the foveola upper: $73\% \pm 4\%$, lower: $68\% \pm 9\%$; two-tailed paired *t*-test: $t(11) = 1.62$, $p = 0.13$; BF = 1.25 for the null hypothesis; Cohen's $d = 0.51$) and the parafovea [upper: $65\% \pm 8\%$, lower: $73\% \pm 13\%$; two-tailed paired *t*-test: $t(7) = -2.00$, $p = 0.085$; BF = 0.78 for the null hypothesis; Cohen's $d = 0.65$]. This result is consistent with findings in the parafovea and perifovea (Carrasco et al., 2001; Cameron et al., 2002; Corbett and Carrasco, 2011; Abrams et al., 2012; Baldwin et al., 2012; Barbot et al., 2021).

Discussion

It is typical to characterize extrafoveal vision at different eccentricities rather than as a whole, as many functions gradually

decrease as stimulus information is presented more peripherally (Anstis, 1974; Robson and Graham, 1981; Pointer and Hess, 1989; see Strasburger et al., 2011; Anton-Erxleben and Carrasco, 2013 for reviews). However, examining foveolar vision as a whole is common practice. Whereas this may seem justified by the fact that the central fovea covers only a tiny (<0.01%) portion of the visual field, it is at odds with the fact that the foveola is vastly overrepresented in the primary visual cortex, which dedicates 8% of its surface area to the processing of the visual input coming from this region (Azzopardi and Cowey, 1993). Moreover, cone density (Curcio et al., 1990; Cooper et al., 2016; Reiniger et al., 2021) and fine visual discrimination (Poletti et al., 2013; Intoy and Rucci, 2020) have been shown to decline just a few arcminutes away from the preferred retinal locus (PRL) of fixation. Therefore, foveolar vision is less homogeneous than usually assumed.

Here, we show that foveolar vision not only changes with eccentricity but also varies around the polar angles of the visual field projecting onto this region, as is the case extrafoveally (see Himmelberg et al., 2023 for a review). Specifically, we found that discriminating stimuli located degrees below, compared to above, the center of gaze is easier, whereas discriminating stimuli just a few arcminutes below versus above the center of gaze proves more challenging. This foveal asymmetry, although comparable in magnitude, is opposite in direction to the corresponding asymmetry in the extrafoveal visual field. In general, the overall shape of the parafoveal performance field is oblong along the horizontal meridian, whereas the foveolar performance field is primarily enhanced along the upper vertical meridian.

The HVA has been reported in parafovea and perifovea studies (Carrasco et al., 2001; Cameron et al., 2002; Levine and McAnany, 2005; Fuller et al., 2008; Montaser-Kouhsari and Carrasco, 2009; Corbett and Carrasco, 2011; Abrams et al., 2012; Baldwin et al., 2012; Greenwood et al., 2017; Himmelberg et al., 2020; Barbot et al., 2021; Kwak et al., 2023; Hanning et al., 2024; Tünçok et al., 2025a). Notably, this parafoveal asymmetry is more prominent in this study than in many previous studies. This difference may be due to differences in stimulus parameters—stimuli used in previous work are larger and often limited to specific spatial frequencies—and the presence of the placeholders, which could have been perceived as distractors—as asymmetries become more pronounced with distractors (Carrasco et al., 2001; Purokayastha et al., 2021). Ultimately, these results show that not only is the foveola characterized by visual asymmetries, but also that these asymmetries are unique in the central most 1° of the visual field.

As discussed in the Introduction, extrafoveal asymmetries are pervasive and have been shown across various visual tasks and stimulus parameters, raising the question of where along the visual processing pipeline these asymmetries emerge. The first factor that could influence the visual asymmetries are the optics of the eye. Optical aberrations are not symmetric along the visual field meridians (Charman and Atchison, 2009), and horizontal/vertical astigmatism and coma vary as a function of polar angle (Pusti et al., 2023). Specifically, the magnitude of vertical coma gradually decreases from the inferior to superior retina (across -18° to 18°), resulting in more optical distortion from vertical coma in the upper compared to the lower vertical meridian (Pusti et al., 2023). In addition to optical factors, at the anatomical level, the extrafoveal retina is characterized by higher cone (Curcio et al., 1987; Song et al., 2011; Wells-Gray et al., 2016; Legras et al., 2018) and retinal ganglion cell (Watson, 2014) density along the horizontal than the vertical meridian. Whereas retinal cone density contributes toward the HVA, no difference in cone density has been reported along the vertical meridian. However, the density of mid-peripheral retinal ganglion cells (mRGCs) is higher along the superior retina, which projects to the lower visual field, compared to the inferior retina (Watson, 2014). Moreover, in the mid-periphery, the convergence of cones to mRGCs is minimal along the horizontal meridian but is the greatest along the inferior retina (Watson, 2014), resulting in greater information loss for stimuli in the upper visual field. This difference aligns with behavioral evidence from this and previous studies.

A computational observer model, however, has shown that optical and retinal factors account for about 40% of the behavioral horizontal-vertical asymmetry and about 10% of the behavioral VMA, and that they are amplified at later processing stages in the visual cortex (Kupers et al., 2019, 2022). In the primary

visual cortex asymmetric differences in BOLD response (Liu et al., 2006), pRF size (Silva et al., 2018), and cortical surface area (Benson et al., 2021; Himmelberg et al., 2021, 2022) have been reported (for a review see Himmelberg et al., 2023). Specifically, for a given eccentricity range, the horizontal meridian can have up to 80% greater cortical surface area than the vertical meridian, and a similar pattern is seen for the lower versus upper vertical meridian (Himmelberg et al., 2021, 2022, 2023). Although further investigation is necessary to elucidate the degree to which the visual cortex influences perceptual asymmetries, factors from the retina to the cortex increasingly contribute to the reported visual asymmetries.

What factors influence foveal asymmetries? Unlike in the extrafovea, optical aberrations in the foveola are constant (Liang et al., 1997; Atchison et al., 2006; Bedggood et al., 2008). Therefore, we can exclude the influence of optics on foveolar asymmetries. However, retinal factors could play a role in shaping these perceptual asymmetries. mRGC have a 1:1 mapping with retinal cone cells (Kolb et al., 1995), and thus neither mRGC density nor cone-to-mRGC convergence should impact the pattern of asymmetries. It has been observed that the foveola exhibits similar asymmetries in cone density to those in the extrafoveal retina, with a higher cone density along the horizontal than the vertical meridian (Curcio et al., 1987; Reiniger et al., 2021). This is consistent with our findings that fine visual discrimination is better along the horizontal versus the vertical meridian. However, like in extrafovea, the foveola shows no differences in cone density along the vertical meridian (Reiniger et al., 2021). Therefore, cone density alone cannot account for the visual asymmetries observed in the foveola.

Importantly, changes in cone density with eccentricity are generally defined with respect to the peak cone density (PCD) location. However, this location does not coincide with the retinal projection of the center of gaze. The center of gaze on the retina is considered as the PRL of fixation, which can be quantitatively defined as the median retinal location of a stimulus during fixation. Notably, there is an offset between the PRL and the point of highest cone density (Putnam et al., 2005; Li et al., 2010; Wilk et al., 2017; Wang et al., 2019; Bowers et al., 2021; Domdei et al., 2021; Kilpeläinen et al., 2021; Reiniger et al., 2021). Specifically, the PRL is shifted nasally and superiorly from the cone density centroid (CDC)—the centroid of the region with highest cone density—by approximately 5 arcmin (Reiniger et al., 2021). Although this is a small shift, it introduces systematic asymmetries in cone density between the superior versus inferior retina. Therefore, if eccentricity is defined with respect to PRL rather than from the CDC location, cone density is higher along the inferior retina, corresponding to the upper visual field, than along the superior retina. Although the overall performance was comparable at the intercardinal locations, in part due to relatively large individual variability, this difference in cone density below versus above the PRL could potentially contribute to the VMA observed in the foveola. It is likely that subsequent stages of processing in the visual cortex further contribute to the foveolar perceptual asymmetries. Yet currently, unlike in extrafoveal vision, nothing is known about possible cortical asymmetries in the processing of foveolar visual input.

The enhanced fine visual discrimination observed in the upper compared to the lower vertical meridian within the foveola may be linked to asymmetries in subcortical visual input representation, particularly in the superior colliculus (SC). In non-human primates, it has been shown that SC neurons representing the upper visual field have smaller receptive fields, are more finely

tuned to spatial structure, and are more sensitive to contrast than those representing the lower visual field (Hafed and Chen, 2016). These asymmetries are more pronounced at larger eccentricities than at the fovea. Interestingly, although this pattern contrasts with the direction of asymmetries observed extrafoveally in humans, it aligns with perceptual asymmetries reported in macaques. Recent findings demonstrate that while humans exhibit poorer extrafoveal sensitivity at the upper vertical meridian, macaques show the opposite pattern (Tünçok et al., 2025b). These studies suggest that humans may possess a distinct SC representation of the visual input, possibly with an even more pronounced upper-lower meridian difference in the fovea than in non-human primates. Such asymmetries could underlie the behavioral differences observed in the present study. Supporting this possibility, it has been shown that the human SC overrepresents the horizontal meridian compared to the vertical meridian in extrafoveal vision (Schneider and Kastner, 2005), consistent with perceptual horizontal-vertical asymmetries reported both here and in previous research (Carrasco et al., 2001; Levine and McAnany, 2005; Fuller et al., 2008; Montaser-Kouhsari and Carrasco, 2009; Schwarzkopf, 2019; Himmelberg et al., 2020; Chakravarthi et al., 2022; Kwak et al., 2023).

Visual sensitivity differences at isoeccentric locations along different directions may serve functional purposes in vision. A horizontal enhancement could be beneficial for socialization with other people at the same height range as faces are commonly located along the horizontal meridian. This asymmetry is also advantageous for reading, both in the fovea and parafovea, as humans can extract words 12–15 letters ahead of the fixated word along the horizontal meridian (Rayner et al., 2010; Justino and Kolinsky, 2023). Interestingly, the HVA is present in both children and adults (Carrasco et al., 2022), suggesting that it may develop early in life or even be present from birth. However, the VMA is absent in children, both in behavior (Carrasco et al., 2022) and cortical surface area (Himmelberg and Tünçok, 2024); behaviorally, it emerges in adolescence (Carrasco et al., 2022). A lower vertical visual field enhancement might be beneficial as the objects that we typically interact with are usually located below our center of gaze (Previc, 1990); however, they are no longer present at intercardinal locations (Carrasco et al., 2001; Cameron et al., 2002; Abrams et al., 2012; Baldwin et al., 2012; Barbot et al., 2021; Purokayastha et al., 2021).

The results of this study also raise important questions about the role of attention in shaping foveal asymmetries—specifically, whether fine-scale attentional allocation can modulate or even eliminate these asymmetries. In the extrafovea, exogenous attention enhances sensitivity uniformly across isoeccentric locations, thereby preserving the magnitude and pattern of visual asymmetries (Carrasco et al., 2001; Cameron et al., 2002; Roberts et al., 2016, 2018). Interestingly, although endogenous attention allows for more flexible deployment (Barbot et al., 2012; Barbot and Carrasco, 2017), it too has been shown to enhance performance uniformly across the visual field (Purokayastha et al., 2021; Tünçok et al., 2025a), suggesting that covert spatial attention distributes resources evenly across locations, regardless of meridional orientation in the extrafovea. Whether this principle extends to the foveola remains unclear. While attention can be selectively directed at this fine spatial scale (Poletti et al., 2017; Guzhang et al., 2021), it is not known whether it operates uniformly—as in the extrafovea—or whether it can be deployed more flexibly to compensate for lower sensitivity in the lower vertical meridian.

In conclusion, using a high-precision eyetracker to investigate visual performance at selected locations across the 1° foveola, this

study revealed that foveolar vision is characterized by visual asymmetries in fine visual discrimination. Whereas the magnitude of the horizontal-vertical asymmetry was attenuated compared to the corresponding parafoveal asymmetry, the magnitude of the asymmetry along the vertical meridian (i.e., upper vs lower) was comparable in both conditions. Remarkably, however, the direction of the vertical asymmetry was reversed in the fovea indicating that distinct mechanisms are at play at this scale. This difference may be the result of fixation behavior leading to changes in cone sampling above vs below the fixated location, given the slight offset between the PCD location on the retina and the PRL, or it may arise from a different cortical representation of foveal input at the level of V1 and beyond. Importantly, these results further emphasize the need to consider foveal vision not as a uniform entity, but as one characterized by significant non-uniformities that shape perception of fine detail.

References

- Abrams J, Nizam A, Carrasco M (2012) Isoeccentric locations are not equivalent: the extent of the vertical meridian asymmetry. *Vision Res* 52:70–78.
- Anstis SM (1974) Chart demonstrating variations in acuity with retinal position. *Vision Res* 14:589–592.
- Anton-Erxleben K, Carrasco M (2013) Attentional enhancement of spatial resolution: linking behavioural and neurophysiological evidence. *Nat Rev Neurosci* 14:188–200.
- Atchison DA, Pritchard N, Schmid KL (2006) Peripheral refraction along the horizontal and vertical visual fields in myopia. *Vision Res* 46:1450–1458.
- Azzopardi P, Cowey A (1993) Preferential representation of the fovea in the primary visual cortex. *Nature* 361:719–721.
- Baldwin AS, Meese TS, Baker DH (2012) The attenuation surface for contrast sensitivity has the form of a witch's hat within the central visual field. *J Vis* 12:23–23.
- Barbot A, Landy MS, Carrasco M (2012) Differential effects of exogenous and endogenous attention on second-order texture contrast sensitivity. *J Vis* 12:6–6.
- Barbot A, Xue S, Carrasco M (2021) Asymmetries in visual acuity around the visual field. *J Vis* 21:2–2.
- Barbot A, Carrasco M (2017) Attention modifies spatial resolution according to task demands. *Psychol Sci* 28:285–296.
- Bedggood P, Daaboul M, Ashman R, Smith G, Metha A (2008) Characteristics of the human isoplanatic patch and implications for adaptive optics retinal imaging. *J Biomed Opt* 13:024008–024008.
- Benson NC, et al. (2018) The human connectome project 7 tesla retinotopy dataset: description and population receptive field analysis. *J Vis* 18:23–23.
- Benson NC, Kupers ER, Barbot A, Carrasco M, Winawer J (2021) Cortical magnification in human visual cortex parallels task performance around the visual field. *Elife* 10:e67685.
- Benson NC, Yoon JM, Forenzo D, Engel SA, Kay KN, Winawer J (2022) Variability of the surface area of the v1, v2, and v3 maps in a large sample of human observers. *J Neurosci* 42:8629–8646.
- Bowers NR, Gautier J, Lin S, Roorda A (2021) Fixational eye movements in passive versus active sustained fixation tasks. *J Vis* 21:16–16.
- Cameron EL, Tai JC, Carrasco M (2002) Covert attention affects the psychometric function of contrast sensitivity. *Vision Res* 42:949–967.
- Carrasco M, Talgar CP, Cameron EL (2001) Characterizing visual performance fields: effects of transient covert attention, spatial frequency, eccentricity, task and set size. *Spat Vis* 15:61–75.
- Carrasco M, Roberts M, Myers C, Shukla L (2022) Visual field asymmetries vary between children and adults. *Curr Biol* 32:R509–R510.
- Carrasco M, Frieder KS (1997) Cortical magnification neutralizes the eccentricity effect in visual search. *Vision Res* 37:63–82.
- Chakravarthi R, Papadaki D, Krajnik J (2022) Visual field asymmetries in numerosity processing. *Atten Percept Psychophys* 84:2607–2622.
- Charman WN, Atchison DA (2009) Decentred optical axes and aberrations along principal visual field meridians. *Vision Res* 49:1869–1876.
- Cherici C, Kuang X, Poletti M, Rucci M (2012) Precision of sustained fixation in trained and untrained observers. *J Vis* 12:31–31.

- Coates DR, Chin JM, Chung ST (2013) Factors affecting crowded acuity: eccentricity and contrast. *Optom Vis Sci* 90:628–638.
- Cooper RF, Wilk MA, Tarima S, Carroll J (2016) Evaluating descriptive metrics of the human cone mosaic. *Invest Ophthalmol Vis Sci* 57:2992–3001.
- Corbett JE, Carrasco M (2011) Visual performance fields: frames of reference. *PLoS One* 6:e24470.
- Cowey A, Rolls E (1974) Human cortical magnification factor and its relation to visual acuity. *Exp Brain Res* 21:447–454.
- Curcio CA, Sloan Jr KR, Packer O, Hendrickson AE, Kalina RE (1987) Distribution of cones in human and monkey retina: individual variability and radial asymmetry. *Science* 236:579–582.
- Curcio CA, Sloan KR, Kalina RE, Hendrickson AE (1990) Human photoreceptor topography. *J Comp Neurol* 292:497–523.
- Danckert J, Goodale MA (2001) Superior performance for visually guided pointing in the lower visual field. *Exp Brain Res* 137:303–308.
- Deubel H, Schneider WX (1996) Saccade target selection and object recognition: evidence for a common attentional mechanism. *Vision Res* 36:1827–1837.
- Domdei N, Reiniger JL, Holz FG, Harmening WM (2021) The relationship between visual sensitivity and eccentricity, cone density and outer segment length in the human foveola. *Invest Ophthalmol Vis Sci* 62:31–31.
- Dumoulin SO, Wandell BA (2008) Population receptive field estimates in human visual cortex. *Neuroimage* 39:647–660.
- Fernández A, Denison R, Carrasco M (2018) Temporal attention improves perception at foveal and parafoveal locations equally. *J Vis* 18:1026–1026.
- Fuller S, Rodriguez RZ, Carrasco M (2008) Apparent contrast differs across the vertical meridian: visual and attentional factors. *J Vis* 8:16–16.
- Fuller S, Carrasco M (2009) Perceptual consequences of visual performance fields: the case of the line motion illusion. *J Vis* 9:13–13.
- Greenwood JA, Szinte M, Sayim B, Cavanagh P (2017) Variations in crowding, saccadic precision, and spatial localization reveal the shared topology of spatial vision. *Proc Natl Acad Sci U S A* 114:E3573–E3582.
- Guzhang Y, Shelchkova N, Ezzo R, Poletti M (2021) Transient perceptual enhancements resulting from selective shifts of exogenous attention in the central fovea. *Curr Biol* 31:2698–2703.
- Guzhang Y, Shelchkova N, Clark AM, Poletti M (2024) Ultra-fine resolution of pre-saccadic attention in the fovea. *Curr Biol* 34:147–155.
- Hafed ZM (2013) Alteration of visual perception prior to microsaccades. *Neuron* 77:775–786.
- Hafed ZM, Chen CY, Tian X (2015) Vision, perception, and attention through the lens of microsaccades: mechanisms and implications. *Front Syst Neurosci* 9:167.
- Hafed ZM, Chen CY (2016) Sharper, stronger, faster upper visual field representation in primate superior colliculus. *Curr Biol* 26:1647–1658.
- Hanning NM, Jonikaitis D, Deubel H, Szinte M (2016) Oculomotor selection underlies feature retention in visual working memory. *J Neurophysiol* 115:1071–1076.
- Hanning NM, Himmelberg MM, Carrasco M (2022) Presaccadic attention enhances contrast sensitivity, but not at the upper vertical meridian. *iScience* 25:103851.
- Hanning NM, Himmelberg MM, Carrasco M (2024) Presaccadic attention depends on eye movement direction and is related to v1 cortical magnification. *J Neurosci* 44:e1023232023.
- Himmelberg MM, Winawer J, Carrasco M (2020) Stimulus-dependent contrast sensitivity asymmetries around the visual field. *J Vis* 20:18–18.
- Himmelberg MM, Kurzwaski JW, Benson NC, Pelli DG, Carrasco M, Winawer J (2021) Cross-dataset reproducibility of human retinotopic maps. *Neuroimage* 244:118609.
- Himmelberg MM, Winawer J, Carrasco M (2022) Linking individual differences in human primary visual cortex to contrast sensitivity around the visual field. *Nat Commun* 13:3309.
- Himmelberg MM, Tünçök E, Gomez J, Grill-Spector K, Carrasco M, Winawer J (2023) Comparing retinotopic maps of children and adults reveals a late-stage change in how v1 samples the visual field. *Nat Commun* 14:1561.
- Himmelberg MM, Winawer J, Carrasco M (2023) Polar angle asymmetries in visual perception and neural architecture. *Trends Neurosci* 46:445–448.
- Holmqvist K, Blignaut P (2020) Small eye movements cannot be reliably measured by video-based p-cr eye-trackers. *Behav Res Methods* 52:2098–2121.
- Horton JC, Hoyt WF (1991) The representation of the visual field in human striate cortex: a revision of the classic holmes map. *Arch Ophthalmol* 109:816–824.
- Intoy J, Rucci M (2020) Finely tuned eye movements enhance visual acuity. *Nat Commun* 11:795.
- Jigo M, Tavdy D, Himmelberg MM, Carrasco M (2023) Cortical magnification eliminates differences in contrast sensitivity across but not around the visual field. *Elife* 12:e84205.
- Justino J, Kolinsky R (2023) Eye movements during reading in beginning and skilled readers: impact of reading level or physiological maturation? *Acta Psychol (Amst)* 236:103927.
- Kilpeläinen M, Putnam NM, Ratnam K, Roorda A (2021) The retinal and perceived locus of fixation in the human visual system. *J Vis* 21:9.
- Kolb H, Fernandez E, Nelson R (1995) Webvision: the organization of the retina and visual system. [Internet].
- Kupers ER, Carrasco M, Winawer J (2019) Modeling visual performance differences ‘around’ the visual field: a computational observer approach. *PLoS Comput Biol* 15:e1007063.
- Kupers ER, Benson NC, Carrasco M, Winawer J (2022) Asymmetries around the visual field: from retina to cortex to behavior. *PLoS Comput Biol* 18:e1009771.
- Kwak Y, Hanning NM, Carrasco M (2023) Presaccadic attention sharpens visual acuity. *Sci Rep* 13:2981.
- Kwak Y, Lu ZL, Carrasco M (2024) How the window of visibility varies around polar angle. *J Vis* 24:1–16.
- Legras R, Gaudric A, Woog K (2018) Distribution of cone density, spacing and arrangement in adult healthy retinas with adaptive optics flood illumination. *PLoS One* 13:e0191141.
- Levine MW, McAnany JJ (2005) The relative capabilities of the upper and lower visual hemifields. *Vision Res* 45:2820–2830.
- Li KY, Tiruveedhula P, Roorda A (2010) Intersubject variability of foveal cone photoreceptor density in relation to eye length. *Invest Ophthalmol Vis Sci* 51:6858–6867.
- Liang J, Williams DR, Miller DT (1997) Supernormal vision and high-resolution retinal imaging through adaptive optics. *J Opt Soc Am A Opt Image Sci Vis* 14:2884–2892.
- Liu T, Heeger DJ, Carrasco M (2006) Neural correlates of the visual vertical meridian asymmetry. *J Vis* 6:12–12.
- Mackeben M (1999) Sustained focal attention and peripheral letter recognition. *Spat Vis* 12:51–72.
- Millodot M, Johnson CA, Lamont A, Leibowitz HW (1975) Effect of dioptrics on peripheral visual acuity. *Vision Res* 15:1357–1362.
- Montaser-Kouhsari L, Carrasco M (2009) Perceptual asymmetries are preserved in short-term memory tasks. *Atten Percept Psychophys* 71:1782–1792.
- Ohl S, Kroell LM, Rolfs M (2024) Saccadic selection in visual working memory is robust across the visual field and linked to saccade metrics: evidence from nine experiments and more than 100,000 trials. *J Exp Psychol Gen* 153:544.
- Palmieri H, Fernández A, Carrasco M (2023) Microsaccades and temporal attention at different locations of the visual field. *J Vis* 23:6–6.
- Pointer J, Hess R (1989) The contrast sensitivity gradient across the human visual field: with emphasis on the low spatial frequency range. *Vision Res* 29:1133–1151.
- Poletti M, Listorti C, Rucci M (2013) Microscopic eye movements compensate for nonhomogeneous vision within the fovea. *Curr Biol* 23:1691–1695.
- Poletti M, Rucci M, Carrasco M (2017) Selective attention within the foveola. *Nat Neurosci* 20:1413–1417.
- Poletti M, Rucci M (2016) A compact field guide to the study of microsaccades: challenges and functions. *Vision Res* 118:83–97.
- Previc FH (1990) Functional specialization in the lower and upper visual fields in humans: its ecological origins and neurophysiological implications. *Behav Brain Sci* 13:519–542.
- Purokayastha S, Roberts M, Carrasco M (2021) Voluntary attention improves performance similarly around the visual field. *Atten Percept Psychophys* 83:2784–2794.
- Pusti D, Kendrick CD, Wu Y, Ji Q, Jung HW, Yoon G (2023) Widefield wavefront sensor for multidirectional peripheral retinal scanning. *Biomed Opt Express* 14:4190–4204.
- Putnam NM, Hofer HJ, Doble N, Chen L, Carroll J, Williams DR (2005) The locus of fixation and the foveal cone mosaic. *J Vis* 5:3–3.
- Randall HG, Brown DJ, Sloan LL (1966) Peripheral visual acuity. *Arch Ophthalmol* 75:500–504.
- Rayner K, Slattery TJ, Bélanger NN (2010) Eye movements, the perceptual span, and reading speed. *Psychon Bull Rev* 17:834–839.
- Reiniger JL, Domdei N, Holz FG, Harmening WM (2021) Human gaze is systematically offset from the center of cone topography. *Curr Biol* 31:4188–4193.

- Rijsdijk J, Kroon J, Van der Wildt G (1980) Contrast sensitivity as a function of position on the retina. *Vision Res* 20:235–241.
- Roberts M, Cymerman R, Smith RT, Kiorpes L, Carrasco M (2016) Covert spatial attention is functionally intact in amblyopic human adults. *J Vis* 16:30–30.
- Roberts M, Ashinoff BK, Castellanos FX, Carrasco M (2018) When attention is intact in adults with ADHD. *Psychon Bull Rev* 25:1423–1434.
- Robson JG, Graham N (1981) Probability summation and regional variation in contrast sensitivity across the visual field. *Vision Res* 21:409–418.
- Rovamo J, Virsu V (1979) An estimation and application of the human cortical magnification factor. *Exp Brain Res* 37:495–510.
- Rucci M, Poletti M (2015) Control and functions of fixational eye movements. *Annu Rev Vis Sci* 1:499–518.
- Santini F, Redner G, Iovin R, Rucci M (2007) Eyeris: a general-purpose system for eye-movement-contingent display control. *Behav Res Methods* 39:350–364.
- Schneider KA, Kastner S (2005) Visual responses of the human superior colliculus: a high-resolution functional magnetic resonance imaging study. *J Neurophysiol* 94:2491–2503.
- Schwarzkopf DS (2019) Size perception biases are temporally stable and vary consistently between visual field meridians. *Iperception* 10:2041669519878722.
- Shelchikova N, Poletti M (2020) Modulations of foveal vision associated with microsaccade preparation. *Proc Natl Acad Sci U S A* 117:11178–11183.
- Silva MF, Brascamp JW, Ferreira S, Castelo-Branco M, Dumoulin SO, Harvey BM (2018) Radial asymmetries in population receptive field size and cortical magnification factor in early visual cortex. *Neuroimage* 167:41–52.
- Song H, Chui TYP, Zhong Z, Elsner AE, Burns SA (2011) Variation of cone photoreceptor packing density with retinal eccentricity and age. *Invest Ophthalmol Vis Sci* 52:7376–7384.
- Stanislaw H, Todorov N (1999) Calculation of signal detection theory measures. *Behav Res Methods Instrum Comput* 31:137–149.
- Strasburger H, Rentschler I, Harvey Jr LO (1994) Cortical magnification theory fails to predict visual recognition. *Eur J Neurosci* 6:1583–1588.
- Strasburger H, Rentschler I, Jüttner M (2011) Peripheral vision and pattern recognition: a review. *J Vis* 11:13–13.
- Talgar CP, Carrasco M (2002) Vertical meridian asymmetry in spatial resolution: visual and attentional factors. *Psychon Bull Rev* 9:714–722.
- Tünçok E, Carrasco M, Winawer J (Forthcoming, 2025a). Spatial attention alters visual cortical representation during target anticipation. *Nat Commun*.
- Tünçok E, Kiorpes L, Carrasco M (2025b) Opposite asymmetry in visual perception of humans and macaques. *Curr Biol* 35:681–687.e4.
- Wang Y, Bensaid N, Tiruveedhula P, Ma J, Ravikumar S, Roorda A (2019) Human foveal cone photoreceptor topography and its dependence on eye length. *Elife* 8:e47148.
- Wang Z, Murai Y, Whitney D (2020) Idiosyncratic perception: a link between acuity, perceived position and apparent size. *Proc Biol Sci* 287:20200825.
- Watson AB (2014) A formula for human retinal ganglion cell receptive field density as a function of visual field location. *J Vis* 14:15–15.
- Wells-Gray E, Choi S, Bries A, Doble N (2016) Variation in rod and cone density from the fovea to the mid-periphery in healthy human retinas using adaptive optics scanning laser ophthalmoscopy. *Eye* 30:1135–1143.
- Westheimer G (1979) Scaling of visual acuity measurements. *Arch Ophthalmol* 97:327–330.
- Wilk MA, Dubis AM, Cooper RF, Summerfelt P, Dubra A, Carroll J (2017) Assessing the spatial relationship between fixation and foveal specializations. *Vision Res* 132:53–61.
- Wright M, Johnston A (1983) Spatiotemporal contrast sensitivity and visual field locus. *Vision Res* 23:983–989.
- Wu RJ, Clark AM, Cox MA, Intoy J, Jolly PC, Zhao Z, Rucci M (2023) High-resolution eye-tracking via digital imaging of Purkinje reflections. *J Vis* 23:4–4.